Mapping Forest Background Reflectance in a Boreal Region Using Multiangle Compact Airborne Spectrographic Imager Data

Jan Pisek, Jing M. Chen, John R. Miller, James R. Freemantle, Jouni I. Peltoniemi, and Anita Simic

***Abstract*—Forest background, consisting of understory, moss, litter, and soil, contributes significantly to optical remote sensing signals from forests in the boreal region. In this paper, we present results of background reflectance retrieval from multiangle high-resolution Compact Airborne Spectrographic Imager sensor data over a boreal forest area near Sudbury, ON, Canada. Modifications of the background by white and black plastic sheets at two sites provide two extreme limits for the development and testing of an algorithm for retrieving the background information from multiangle data. Measured background reflectances in red and near-infrared bands at six sites in the vicinity of these modified sites are used to validate the algorithm. We also explore the effect of uncertainties in the input forest structural parameters on this retrieval. The results document: 1) capability of the algorithm to retrieve meaningful background reflectance values for various forest stand conditions, particularly in the low to intermediate canopy density range; 2) the effect of background bidirectional reflectance distribution function on retrieved values; 3) performance of the algorithm using data with different cross angle values; and 4) verification of the internal consistency of the geometric-optical 4-Scale model used. The results provide an important platform for the operational estimation of the vegetation background reflectance from the bidirectional reflections observed by the Multiangle Imaging Spectroradiometer instrument.**

***Index Terms*—Background reflectance, Compact Airborne Spectrographic Imager (CASI), Finnish Geodetic Institute Field Goniospectrometer, multiangle remote sensing, understory.**

I. Introduction

LEAF AREA index (LAI), defined as one half of the total green leaf area per unit horizontal ground surface area [1] after [2], is a key surface characteristic for modeling carbon, water, and energy exchanges between the Earth surface and the atmosphere. Since ecosystem models are often applied over large areas, much attention has been paid to the estimation of LAI using remote sensing data [3], [4]. The typical approach is to place the emphasis on determining the relationship between LAI and the canopy optical properties, and the properties of understory/ground layer are given as an input based on simplifying assumptions [5]. However, the validation of various LAI products derived from remote sensing data has revealed the importance of background reflectance on the accuracy of canopy LAI estimation [6]–[11]. Lang *et al.* [12] observed higher correlation between stand reflectances and LAI for forests with higher canopy cover with the understory increasingly obscured and its contribution to stand reflectance reduced. Rautainen and Stenberg [13] reported that the contribution of understory reflectance can range up to 95% for LAI below 0.5. Previous LAI validation efforts have resulted in the recognition that understory cannot be neglected in reflectance modeling [14], particularly in the case of low to intermediate canopy cover. Unifying the definitions by [5], [15], and [16], by the term forest background, we refer to all the materials below the forest canopy such as understory vegetation, leaf litter, grass, lichen, moss, rock, soil, snow, or their mixtures, which are detectable through the overstorey canopy from above.

Few approaches have been suggested to account for, or minimize, the variable understory effect on the stand reflectance. In the majority of forest reflectance models, the background reflectance is given by a fixed value at each wavelength [17] or modeled bidirectional reflectance distribution function (BRDF) [18] using field observations [19]. Kuusk *et al.* [20] proposed the understory spectra to be estimated from forestry databases or spectral data banks. Peltoniemi *et al.* [21] reported their initial efforts to create such a spectral data bank for the most common understory species in Finland. However, if we consider large areas on a continental or global scale, such an approach would be tremendously demanding with regard even to account for the common understory types. Several authors also noted the large variations even among the same species [21]–[23]. Seasonal variations of the background composition and their optical properties would present a further challenge.

Alternatively, Deng *et al.* [24] tried to minimize the effect of the background/understory on LAI retrieval for forest stands by developing the relationships using a reduced simple ratio (RSR). However, during the validation of this LAI product, it was noted that the understory effect still might have not been entirely removed [10], [25], and direct inclusion of seasonally variable background vegetation spectra into the algorithms is desirable.

Multiangle remote sensing has been shown to enable us to describe properties of terrestrial surfaces by means that are not

Manuscript received February 1, 2009; revised May 3, 2009. First published August 18, 2009; current version published December 23, 2009. This work was supported by the Natural Science and Engineering Council of Canada (Discovery Grant) and student assistantships of the Centre for Global Change Science at the University of Toronto to the first author.

J. Pisek is with the Department of Geography and Program in Planning, University of Toronto, Toronto, ON M5S 3G3, Canada, and also with Tartu Observatory, 61602 Toravere, Estonia (e-mail: jan.pisek@utoronto.ca).

J. M. Chen and A. Simic are with the Department of Geography and Program in Planning, University of Toronto, Toronto, ON M5S 3G3, Canada (e-mail: chenj@geog.utoronto.ca; simica@geog.utoronto.ca).

J. R. Miller and J. R. Freemantle are with the Department of Earth and Space Science and Engineering, Petrie Science and Engineering Building, York University, Toronto, ON M3J 1P3, Canada (e-mail: jrmiller@yorku.ca; james.freemantle@aerocan.net).

J. I. Peltoniemi is with the Finnish Geodetic Institute, 02431 Masala, Finland (e-mail: jouni.peltoniemi@fgi.fi).

Color versions of one or more of the figures in this paper are available online at http://ieeexplore.ieee.org.

Digital Object Identifier 10.1109/TGRS.2009.2024756

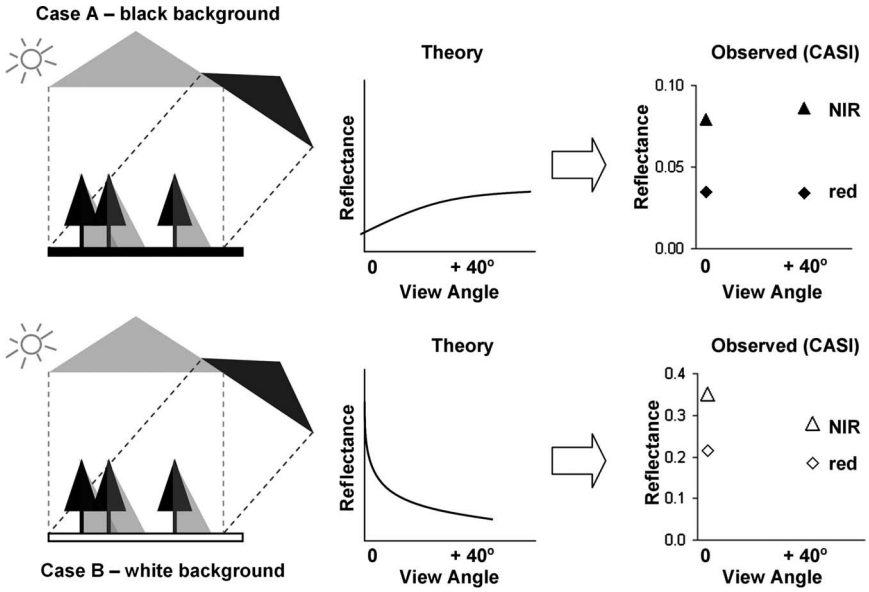

Fig. 1. Theorized and observed variation of the total reflectance of a forest canopy with view zenith angle in red and NIR band for two contrasting background types.

possible using mono-angle data (for the overview of recent progress in the multiangle remote sensing see the review of [26]). Initial studies of the ability of multiangle remote sensing for retrieving background optical properties provided some encouraging results [27], [28]. In particular, Canisius and Chen [27] used the 4-Scale model [29], [30] to examine the feasibility of determining the understory reflectance over a boreal region given two viewing geometries with an inversion approach using Multiangle Imaging Spectroradiometer (MISR) [31] data. Due to the lack of field measurements, the verification of the derived background reflectivity estimates was rather limited. It is therefore highly desirable to acquire high-resolution airborne and *in situ* measurements to further validate the methodology. This validation is a necessary step for us to exploit MISR data for mapping the background reflectance globally, in order to improve our global LAI mapping.

In this paper, we present results of background reflectance retrieval from multiangle high-resolution Compact Airborne Spectrographic Imager (CASI) data for three dominant boreal forest species: black spruce (*Picea mariana*), jack pine (*Pinus banksiana*), and trembling aspen (*Populus tremuloides*). The theory underpinning the proposed algorithm for deriving background reflectance is further investigated by means of modifying and controlling the understory properties. Finally, we carry out simulations to test the inner consistency of the 4-Scale geometrical-optical (GO) model used in this paper and to explore the effect of uncertainties in the input canopy structural parameters on the retrieval of the background reflectance.

II. Methodology

A. Background Reflectivity Retrieval Theory

In GO modeling, the total canopy reflectance is expressed as a linear combination of the contributions from sunlit and shaded crown (R_T and R_{ZT}) and background (R_G and R_{ZG}) components [32], [33]

$$R = R_T \cdot k_T + R_G \cdot k_G + R_{ZT} \cdot k_{ZT} + R_{ZG} \cdot k_{ZG} \quad (1)$$

where k_T, k_G, k_{ZT}, and k_{ZG} are the corresponding proportions of the four components in the instantaneous field of view (IFOV). The contributions of the components to the total reflectance change with view angle as the proportions vary with view angle. Assuming that the sun is at a fixed angle and observations are made along a plane where target reflectances change little with angle, the variation of total reflectance with view angle for a given stand should follow opposite trajectories for two contrasting backgrounds, where one background type is with higher and the other one with lower reflectivity than that of the overlying forest canopy. This concept is shown in Fig. 1. In both scenes (Fig. 1, Cases A and B), the background contribution is the largest at nadir, while the contribution of the overlying forest canopy increases with increasing view zenith angle. The total reflectance increases (Case A) or decreases (Case B) with view angle depending on the background reflectivity. If the background reflectivity is lower than that of the overlying forest canopy (i.e., dark background), the total reflectance increases with view zenith angle; the opposite is true for bright (i.e., white, such as snow) background. We provide the validation of this first step in the theory of the background retrieval in the Results section.

Our algorithm is based on the premise that the reflectance of the overstory and the understory at a given illumination angle changes little between chosen view angles or this change can be well estimated within the algorithm. Forward-scattering reflectances of various targets were shown to be fairly constant [34]–[37], particularly when not too close to the principal plane [21]. The observed reflectance at nadir $(R_{\rm n})$ and at an angle in forward direction $(R_{\rm a})$ can be then described by the following set of equations:

$$R_{\rm n} = R_T \cdot k_{Tn} + R_G \cdot k_{Gn} + R_{ZT} \cdot k_{ZTn} + R_{ZG} \cdot k_{ZGn} \quad (2)$$

$$R_{\rm a} = R_T \cdot k_{Ta} + R_G \cdot k_{Ga} + R_{ZT} \cdot k_{ZTa} + R_{ZG} \cdot k_{ZGa}. \quad (3)$$

Next, shaded components of trees and ground can be expressed as functions of their sunlit parts and the multiple

scattering factor [38]–[40], giving $R_{ZT} = M \cdot R_T$ and $R_{ZG} = M \cdot R_G$, where $M = R_Z/R$ for a reference target, with R_Z representing its shaded reflectance. Solving (2) and (3), the background reflectivity R_G can be then calculated as in (4), shown at the bottom of the page, where the total reflectances $R_{\rm n}$ and $R_{\rm a}$ are acquired from the nadir and a forward direction, M is predetermined by model inversion, and the proportions of the components can be predicted from the GO model. These scene components are estimated using a lookup table constructed with 4-Scale [41], which takes into account their variations with solar and view angles with given LAI and the best estimates of other stand structure parameters such as tree height, crown radius, and stand density, as described in the following section.

B. 4-Scale Model

4-Scale is a GO radiative-transfer model with an emphasis on the structural composition of forest canopies at different scales [29], [30], [41]. From the model output, only the proportions of the components were used in the background reflectance retrieval from the study area. Stand structure in the reflectance model is characterized by trees with internal structures. The nonrandom spatial distribution of trees is simulated using the Neyman type A distribution [42] that creates patchiness of a forest stand. The tree surface created by the crown volume (cone and cylinder, or spheroid) is treated as a complex medium rather than a smooth surface so that shadowed foliage can be observed on the sunlit side and sunlit foliage on the shaded side. Aside from the total reflectance, the model provides the needed outputs of the proportions of sunlit and shaded tree and ground components. Inputs to 4-Scale were obtained directly from the stand parameter measurements described in Section III-A. View and solar angles were specified according to their configuration during individual flights as described in Section III-B.

C. Uncertainty in the Background Reflectance Estimates

Understanding the impact of uncertainty in a retrieved parameter and the following implications is an important part of any algorithm validation effort [43]. Since the ultimate goal of the herein tested methodology is to retrieve the forest background reflectance over large areas where not all canopy parameters are known, we explored the effect of uncertainty in the input canopy parameters on the retrieval of the background reflectance. We chose a method that assessed both the possible bias within the algorithm [(4)] and the amount of bias introduced by factors other than the algorithm in the process of background reflectance retrieval.

The sensitivity of input to 4-Scale and its output was examined by [44]. Compared to LAI, the effects of stand density on the 4-Scale output were small [44]. We created two scenarios to represent the increase of LAI of a forest stand. In one scenario, we keep the stand density constant at 2000 trees/ha while increasing the size of the trees in regular steps. At each step, the vertically projected crown area was calculated. The same crown area coverage was also achieved in the second scenario by keeping tree dimensional parameters constant for all steps while increasing the stand density. Close-to-reality configurations might be then found in the space bounded by these two scenarios for every step. The parameters for each step and scenario are presented in Table IV.

In the first test, the 4-Scale model was run with the input parameters from Table IV for every step of both scenarios and the angular constellation set to correspond to the situation during the CASI flight. The background reflectance was then calculated from (4) with total canopy reflectances and proportions of the components as predicted by the 4-Scale model. If there is no bias in the 4-Scale model and (4), the retrieved background reflectances would not change with increasing canopy foliage, as all the changes in predicted stand reflectances should appear due to changes of the foliage only.

The stand parameters, such as tree height or stand density, might still not be perfectly known during the operational use of the algorithm over large areas despite the promising advances in their retrieval [45]–[48]. The error due to the uncertainty in the input stand parameters was assessed in the second test. The background reflectances were again calculated for every scenario and every step, but the total nadir and angular reflectances were held constant and corresponded to CASI data over one study site with known stand parameters, instead. The proportions of components were the same as in the first test. The comparison of background reflectances allowed us to see the effect of incorrectly specified stand parameters on the results.

III. Study Area

A. Study Sites and Field Measurements

The study sites include four black spruce (labeled SB7, 11, 12, 17), one trembling aspen (AS19), and one young jack pine site (PJ21) located near Sudbury, ON, Canada (Fig. 2). Canopy-Site configurations range from young to mature and from sparse to dense. The understory vegetation at black spruce sites consisted mainly of feather moss (*Hylocomium splendens*) with varying contributions from labrador tea (*Ledum groenlandicum*) and leather leaf (*Chamaedaphne calyculata*). Bare soil was the dominant ground cover at the aspen and young jack pine sites. Sites SB7 and SB11 had two parts with unmodified and modified understory. At the modified sites SB7 and SB11, we cut and removed all understory and covered the ground with white plastic. At SB7, we additionally laid a layer of black plastic. This layer was removed after the first flight and white plastic was exposed for the second flight. The unmodified parts are identified with a subscript B.

Quadratic plots of 30-m side length with a central east–west-oriented transect line were established at each site. Along each transect, a forestry flag was placed every 10 m. At each

$$R_G = \frac{R_{\rm n}(k_{Ta} + k_{ZTa} \cdot M) - R_{\rm a}(k_{Tn} \cdot M)}{-k_{Tn} \cdot k_{Ga} + k_{Gn} \cdot k_{Ta} + M(-k_{Tn} \cdot k_{ZGa} + k_{Gn} \cdot k_{ZTa} - k_{Ga} \cdot k_{ZTn} + k_{Ta} \cdot k_{ZGn}) + M^2(-k_{ZTn} \cdot k_{ZGa} + k_{ZGn} \cdot k_{ZTa})} \quad (4)$$

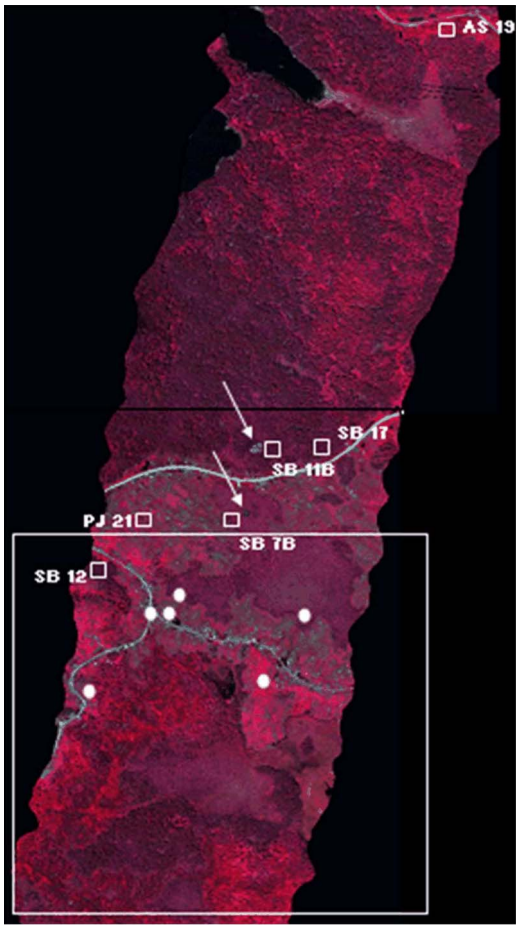

Fig. 2. CASI composite image [(blue) 550 nm, (green) 656 nm, (red) 800 nm in viewing nadir angle of the study area near Sudbury, ON, with indicated sites (for the sites' description please refer to Table I]. Coverage of the background reflectance map from Fig. 8 is depicted by white rectangle.

plot, measurements of forest structural variables and forest background reflectance were carried out within a week of the CASI flight date, June 28, 2007. Stand variables for the sites are summarized in Table I.

The effective LAI (L_e) was measured using the LAI-2000 Plant Canopy Analyzer (LI-COR, Lincoln, NE) instrument. Measurements at each flag along the site transect were taken under diffuse sky conditions (i.e., overcast sky or at dusk). We assessed the multiple scattering effect by comparing L_e based on rings 1–3 (corresponding to the zenith angle range from 0° to 45°) and rings 1–5 (0° to 75°). Interestingly enough, we observed the same average difference between these two ways of L_e calculation (16%) as the previous study [49] for stands collected from the whole of Canada. We have increased by 16% for all L_e values from LAI-2000 calculated using rings 1–5 to account for the multiple scattering effect.

Beyond-shoot clumping (Ω_{E}) was quantified using the element clumping index and measured directly in the field during sunny days along the same transects using the tracing radiation and architecture of canopies instrument (Third Wave Engineering, Ottawa, Canada) based on a canopy gap-size distribution theory [50], [51]. Values of woody-to-total leaf area ratio (α) and needle-to-shoot ratio (γ_{E}) were used as provided by [49] and [52] and were comparable with estimates of [44] for different sites within the same study area.

For the estimation of forest background reflectance, we first took photos around each forest flag with a digital camera pointing perpendicularly to the ground. The sunlit reflectance of the present forest floor types was measured using a FieldSpec Pro spectroradiometer (Analytical Spectral Devices, Inc., Boulder, CO). To capture the interspecies variability as well as the intraspecies variability in spectral reflectance as influenced by different moisture and environmental conditions, we took several sets of spectral reflectance measurements at different locations at each site. All spectral reflectance measurements were taken in the nadir direction under clear sky conditions at a height of about 3 cm above sunlit targets (leaves or moss/lichen layer, ground). The solar position during the understory spectra measurements was consistent with the configuration during CASI flights. The measurements were standardized to reflectance using a Spectralon diffuse reflectance target (Labsphere, North Sutton, NH). The average forest background reflectance for each site was obtained based on the reflectance of the cover types weighted by their area fractions as derived from the photos. Finally, the spectra of plastic sheets were measured in a laboratory with Finnish Geodetic Institute Field Goniospectrometer [53]. The light source was positioned at zenith angle of 38° that corresponded to the sun position during the second flight.

B. CASI Data and Processing

Two CASI flights took place on June 28, 2007 at an altitude of 5000 ft above the ground between 18:10 and 20:38 GMT at the solar zenith angle of 25.2° to 44.3°. CASI was operated in the hyperspectral mode (72 channels; spectral range 408–947 nm; bandwidth 7.5 nm) with 2-m spatial resolution [54]. Variable viewing zeniths were obtained by mounting the camera on a tilting bracket and adjusting the tilt along the flight line. The view zenith angles were 0° (nadir), -30°, and $+40^\circ$ for the first flight, and 0°, -40°, $+40^\circ$, and $+45^\circ$ for the second flight. Following the convention of [14], negative values indicate the backscattering hemisphere and positive values indicate the forward-scattering hemisphere. The view angles for the back-scattering hemisphere were set to be close to solar zenith position during individual flights. Cross angles (absolute angle difference from the principal plane; Φ) varied with flights in order to see the effect of the deviation from the principal plane on the understory reflectance retrieval. Φ was 29° for the first flight and $\Phi = 3^\circ$ for the second flight with the camera set at $\mathrm{VZA} = 40^\circ$. For the view angle of 45° during the second flight, $\Phi = 15^\circ$. In the following text, the results are indicated by the value of the cross angle. Nadir view observations were always taken with $\Phi = 15^\circ$.

The multiangle images were radiometrically calibrated using the latest radiance scale factors for the CASI sensor and atmospherically corrected to at-ground reflectance using Modtran 4 in the PCI atmospheric correction package (PCI Geomatics, Richmond Hill, Canada). Direct measurements of atmospheric parameters were not available during the CASI overflights, however aerosol optical depth was estimated from nearby measurements of visibility. Methodological measurements from Environment Canada gave the conditions as clear with a visibility of 25 km. Other atmospheric parameters were allowed to default to MODTRAN mid summer, mid

TABLE I
CHARACTERISTICS OF THE INVESTIGATED STANDS

site	AS 19	SB 7B	SB 11B	SB 12	SB 17	PJ 21
tree species	trembling aspen	black spruce	black spruce	black spruce	black spruce	young jack pine
latitude	47.1762	47.1616	47.1635	47.1600	47.1638	47.1619
longitude	81.7378	81.7454	81.7452	81.7509	81.7599	81.7490
stand density (trees/ha)	2000	2000	4000	4000	4000	8000
zenith gap fraction	0.11 (25°)	0.51 (27°)	0.08 (39°)	0.06 (39°)	0.12 (40°)	0.44 (59°)
canopy LAI	3.65	2.65	5.5	4.57	4.04	2
element clumping index	0.9	0.73	0.88	0.89	0.81	-
tree height (m)	13.5	5.6	12.7	10.6	15.9	1.8
DBH (cm)	32.3	19.3	27.1	36.9	53	-
understory species	bare soil	feather moss	feather moss	feather moss	feather moss	bare soil
	bush honeysuckle	labrador tea	labrador tea	labrador tea	labrador tea	rotten wood
	labrador tea	leather tea	leather tea	leather tea	dogwood	rock
	hazelnut			lichen	rotten wood	bush honeysuckle
	blunt leaf orchid			rotten wood	leather tea	

latitude values. The reflectance images were geometrically corrected using Itres' geometric correction software (Itres, Calgary, Canada) and roll, pitch, and location information from an on-board navigation system. Geometric correction based on this system was further adjusted using ground control points measured in the field. These ground control points include 2 m $\times$ 2 m white plastic sheets placed on the road sides near the sites, and identifiable ground features such as road crossings, rock outcrops, etc. Geometrically corrected off-nadir images were then registered to the nadir images. The final spatial resolution of the images is 3 m. The roll and pitch were quite pronounced in the off nadir images making geometric correction very difficult. The final RMSE for the whole scenes were 5–6 pixels. However, since all the sites were located close to distinct features (white/black plastic, roads), it has been verified that the reflectance data for various view angles cover nearly identical areas. In addition, the background mapping was not carried out on individual pixels, but on averaged plots of size 30 m $\times$ 30 m (i.e., 100 pixels). If the accuracy could not be guaranteed due to roll and pitch distortions over particular sites in the image, we did not carry out the calculations. All sites were located on flat terrain and there were no topographic effects that needed to be taken into account in our image analysis.

The hyperspectral mode data were finally aggregated to create MISR-like responses for red and NIR bands. We averaged the CASI hyperspectral bands that cover the corresponding MISR red and NIR spectral bandwidths as provided by [31]. The new bands were centered at 671.3 nm (versus 671.7 nm for MISR) and 866.1 nm (versus 866.4 nm for MISR).

IV. RESULTS AND DISCUSSION

A. Changes of Total Reflectance With View Angle

The verification of the predicted total reflectance changes with view angle in the field by modifying the background properties with black and white plastic presented the first important step in our research. To our knowledge, this is for the first time the forest understory has been completely controlled and studied at such a spatial extent (30 m $\times$ 30 m and 20 m $\times$ 20 m plots in stands with different densities). Complete understory removal was previously performed by [55], but the effect of understory was assessed only indirectly via observing the changes in the scene normalized difference vegetation index between pre- and posttreatment IKONOS imagery.

The total reflectances obtained from the CASI data were examined at two viewing angles. The total reflectances increased with view angle for the dark background and decreased for the white background situation for the SB7 site with the modified understory (Fig. 1). This behavior confirmed the first step in the theory of the background reflectance retrieval as described in the Methodology section. The anisotropy factor (AF), calculated by normalizing the reflectance in a specific view direction by nadir reflectance for a given wavelength [56], was more pronounced for both red and NIR band values from the second flight with white plastic background below. The higher AF values were also observed during the second CASI flight over SB11 site, where white background was present for both flights. The angular measurements during the first flight were taken on a plane further away from the principal plane than during the second flight (i.e., $\Phi = 29^\circ$ versus $\Phi = 3^\circ$). Observed behavior of AF values confirms first the reflectances of components (canopy and background) change less with viewing angle on a plane further away from the principal plane, and therefore the data from the first flight are more appropriate for the background reflectance retrieval.

B. Background Reflectance

The retrievals of background reflectance using (4) were validated first over the sites with modified understory. Testing the new algorithm over the control sites revealed important impacts of our algorithm assumption of the Lambertian background. While the CASI-retrieved values were very close to field measurements in both bands in the case of dark background over SB7 (lower stand density), significant disagreement between values in the red band was present over the same site with the white background [Fig. 3(a)]. The percentage error (PE) was 43% and 28%, respectively. Interestingly, all the retrievals in red band over the other modified site SB 11 (higher stand density) were also underestimated, but the error margin was significantly smaller with PE $< 15\%$ [Fig. 3(b)].

Analysis of the complete bidirectional reflectance factors (BRFs) of black and white plastic explains this behavior (Fig. 4). The BRFs of all the plastics have huge specular reflectance. The anisotropy effect is usually the most pronounced along the principal plane [57], and it was shown to decrease with increasing angular distance from the principal plane [58]. The width of the specular reflectance effect along the principal plane varies between the plastics. The effect

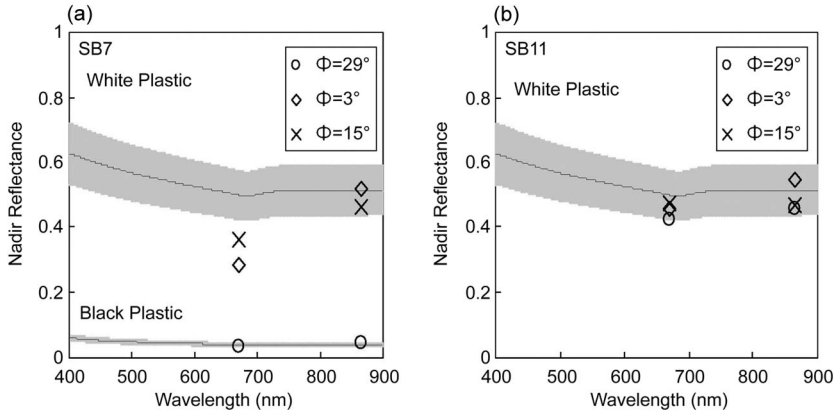

Fig. 3. Nadir reflectance spectra (BRF) from the measurements (lines) and as calculated from CASI data (point markers) for two black spruce stands with modified background. Numbers indicate the angular difference of CASI flights and the principal plane.

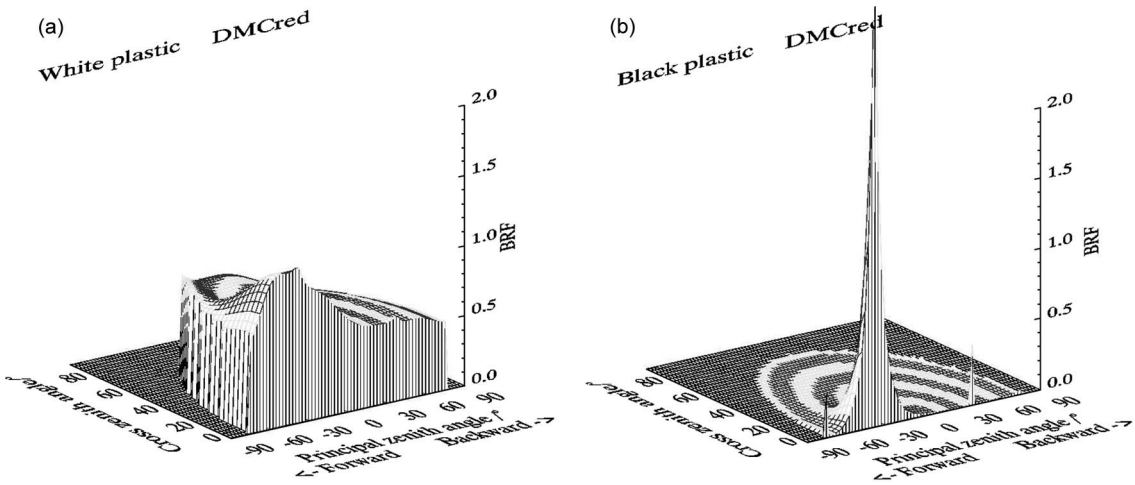

Fig. 4. BRDF of (a) white and (b) black plastic in red band. Lamp zenith angle is 38°. The concentric colored rings clarify zenith angles.

is very narrow for the black plastic, and the black plastic background configuration was observed by CASI camera with $\Phi = 29°$. The background reflectance thus did not change very much with view angle, and the retrieved values were very close to the field measurements. The white plastic background configuration was observed with smaller cross-angle values $\Phi = 3°$ and $\Phi = 15°$. The angles were not enough to avoid the spike in the forward scattering direction due to the specular reflectance, and background reflectances then varied with view angle. The assumption of the Lambertian target was violated, which resulted in biased background reflectance retrievals. If we decreased the total angular reflectance by the percentage difference between the angular and nadir reflectance of the white plastic as measured during the BRF reconstruction of the material in the laboratory, the background reflectance predicted from the algorithm closely matched the one measured in the field. This effect was not so pronounced for SB11 [Fig. 3(b)] due to the higher stand density (twice as high as for SB7). The proportions of visible background were much lower for SB11 and for all angles trees occupied more than half of the IFOV. The background was a dominant component for all angles at SB7. It can be concluded that if the BRDF of the understory is known, the corrections to the algorithm input reflectances can be done to produce true nadir background reflectance. The results might point to a possible lower accuracy of the background reflectance retrieval over very bright surfaces with strong specular reflectance such as snow in winter [59]. However, our initial results with satellite-based MISR data [60] seem to indicate the algorithm can produce meaningful background retrievals over natural areas with snow in winter as well.

The performance of the algorithm over sites with unmodified background is described in Fig. 5 and Table II. The retrievals were validated with field measurements, collected over transect locations at every site. Similar to [21] and [22], sometimes optical spectra measured at nadir at various locations even just a few meters apart could be quite different among the same species. The degree of understory vegetation cover can also vary considerably within one stand [61]. The retrieved background reflectances match reasonably well with the *in situ* measurements in absolute terms, with scatter mainly due to uncertainties in the estimated angular reflectance pattern of the background measured in field, overstory parameterization, and the pixel coregistration. The algorithm seems to perform relatively well for various black spruce, jack pine, and aspen stands. The results indicate the robustness of the algorithm for estimating the forest background reflectance over diverse palettes of understory situations

The availability of the CASI data at different azimuthal angles relative to the sun also permitted a look at the effect of the angular distance from the principal plane on the quality of

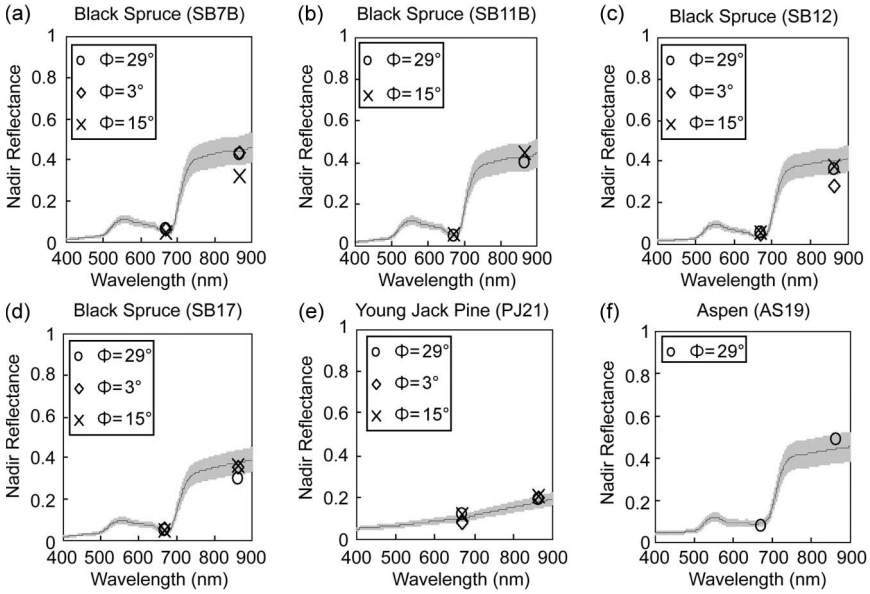

Fig. 5. Nadir reflectance spectra (BRF) from the measurements (lines) and as calculated from CASI data (point markers) for six stands with unmodified background. Numbers indicate the angular difference of CASI flights and the principal plane.

TABLE II
COMPARISON OF MEASURED AND CALCULATED STAND BRF FROM CASI DATA IN RED AND NIR BAND OVER SIX STANDS IN 2007. NUMBERS IN BRACKETS ARE RELATIVE ABSOLUTE ERRORS FROM THE IN-FIELD MEASURED VALUES

		In-situ	View Angle 40°		View Angle 45°
band	site	measurement	Φ = 29°	Φ = 3°	Φ = 15°
red (671 nm)	SB7B	0.0501	0.0610 (0.22)	0.0627 (0.25)	0.0467 (0.07)
	SB11B	0.0513	0.0476 (0.07)		0.0598 (0.17)
	SB12	0.0501	0.0525 (0.05)	0.0455 (0.09)	0.0603 (0.20)
	SB17	0.0506	0.0469 (0.07)	0.0532 (0.05)	0.0452 (0.10)
	PJ21	0.1009	0.1155 (0.14)	0.0773 (0.23)	0.1224 (0.21)
	AS19	0.0927	0.0767 (0.17)		
NIR (866 nm)	SB7B	0.4475	0.4289 (0.04)	0.4340 (0.03)	0.3227 (0.28)
	SB11B	0.4268	0.3980 (0.07)		0.4490 (0.05)
	SB12	0.4028	0.3639 (0.10)	0.2855 (0.29)	0.3817 (0.05)
	SB17	0.3774	0.3010 (0.20)	0.3574 (0.05)	0.3636 (0.04)
	PJ21	0.1782	0.1906(0.12)	0.1993 (0.07)	0.2092 (0.17)
	AS19	0.4444	0.4889 (0.10)		

retrievals. For the analyzed collection of the stands, results were slightly improved with increasing cross angle. Mean PE was the worst for retrievals with $\Phi = 3^\circ$ (16% in red and 12% in NIR) and the best at 12% (red) and 10% (NIR) for retrievals with $\Phi = 29^\circ$. Both these results and the findings from the Section IV-A confirm that angular observations further away from the principal plane are indeed more appropriate for the background reflectance retrieval, in agreement with the proposal of [27] that angular observations near the perpendicular plane would be optimal for background retrieval. This may be due to two reasons: 1) the BRDF effect of the background is minimized and 2) the shadow fraction of the overstorey varies the least along the perpendicular plane. The angular configuration of our CASI measurements near the principal plane was designed for the purpose of clumping index retrieval [62], while the same data are used for background retrieval. Although this configuration is not optimal, it was encouraging to see that the background information can still be reliably retrieved, and this further demonstrates the robustness of our background algorithm.

Our results further suggest that at least for observations with larger sun-view azimuthal angle differences ($\Phi = 29^\circ$ and $\Phi = 15^\circ$), the CASI sensor at smaller view zenith angles delivered slightly more accurate background reflectance retrievals. This is probably caused by larger proportions of background seen at smaller view zenith angles. Although the view zenith angle varied only less than 5° during our CASI acquisition, our results indirectly support findings by [63], who observed smaller contributions from the understory with more oblique viewing angles for CHRIS PROBA data.

Subsequently, a background reflectance map was produced for a subscene of the study area with minimal coregistration errors between two images at different view angles (Fig. 6). The

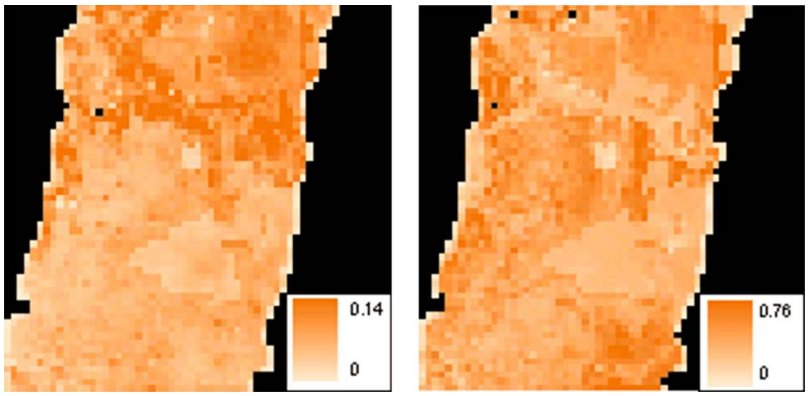

Fig. 6. CASI background reflectance map (left-red band; right-NIR band) over a subset area of the scene from Fig. 2, near Sudbury, ON, Canada. The spatial resolution of the image is 20 × 20 m.

TABLE III
COMPARISON OF MEASURED AND CALCULATED BACKGROUND BRF FROM CASI DATA (JUNE 2007) IN RED AND NIR BAND OVER ADDITIONAL SITES, MEASURED IN JUNE 2008. NUMBERS IN BRACKETS ARE ABSOLUTE RELATIVE ERRORS FROM THE IN-FIELD MEASURED VALUES

site	red band (671 nm)		NIR band (866 nm)	
	in situ	CASI	in situ	CASI
J 0	0.1543	0.1441 (0.07)	0.1872	0.1703 (0.09)
J 1	0.0517	0.0576 (0.12)	0.4233	0.4568 (0.08)
J 2	0.0985	0.0762 (0.23)	0.2418	0.2991 (0.24)
J 3	0.1092	0.0709 (0.35)	0.3405	0.3257 (0.04)
J 4	0.0884	0.0796 (0.10)	0.3380	0.3299 (0.02)
J 5	0.0349	0.0581 (0.67)	0.3746	0.3595 (0.04)

inputs were CASI data from the first flight with $\Phi = 29^\circ$ and the scene proportions calculated for SB11B, since this site was deemed to be the most representative of the stand conditions in the subscene. The area was revisited in late June 2008, and the map was validated with background reflectance measurements at randomly placed sites. The compatibility of the measurements coming from different years (CASI data from June 2007; field data from June 2008) was assured by visiting the transect at SB12 and remeasuring all present understory species. The averaged background site spectral curves for 2007 and 2008 closely agreed with PE of 4%.

Background values were produced only for coniferous stands in the map (deciduous stands were not present in the area). Areas covered with peatland, bare soil, or gravel hold their original nadir reflectances. Table III includes the results of the background map validation. Location J0 corresponds to a road, and the PE of CASI data to the field measurements was under 10% for both red and NIR band. This confirms the minimal effect of atmosphere on the data observed by CASI during the flights over the study area. In agreement with [64], exposed road showed relatively isotropic reflectance characteristics and was bright in all viewing directions. The other sites (J1–J5) corresponded to various coniferous stands (both black spruce and jack pine). The retrievals were again reasonably close to the field measurements with few exceptions in the red band. Overall, background retrievals in the NIR band tend to be more stable than the ones in the red band. This may be due to an effect of higher multiple scattering in NIR that balances out local differences and results in smoother BRDF of these stands.

If the background reflectance signal did not differ from the overstory canopy, the understory effect on the canopy LAI retrievals would not be too high and could have been ignored. Fig. 7 shows the importance of not neglecting the background reflectance. The background reflectances tend to be higher in both the red and the NIR band than the total reflectances. This is because the large shadow fractions at the stand level reduce the overall apparent reflectance from above the stand, while the background reflectance refers to its inherent reflectivity. The relative increase tends to be higher in the red band than in the NIR band, which results in decreased SR values for the background in comparison with the total reflectance at the stand level. Our ground-truth data may still be insufficient for validating the small regional map produced by CASI, but the significant shifts in the spectral space from total reflectance positions in Fig. 7 underline the fact that the background reflectance and the role of understory cannot be ignored in the canopy LAI retrieval.

C. Stand Reflectance Simulations

To gain confidence in our approach, we tested the internal consistency of the 4-Scale model inversions. While the model-predicted stand reflectances were increasing with canopy foliage, the background reflectance, calculated with (4) based solely on the outputs from the model, was staying almost constant (Fig. 8). This behavior confirms that the 4-Scale model itself through the predicted proportions of components introduces only a minimal bias into the calculations of the background reflectance. However, the uncertainties in the input parameters to the model would be other sources of errors.

In this paper, we acquired detailed information about the stand structure. Component proportions could be then predicted fairly well with 4-Scale. What happens if all this stand structure information is not available? The effects of input stand parameters were therefore investigated. Inputs into the (4) were proportions of components as provided by 4-Scale for every step in each scenario; total nadir and angular reflectances were kept constant and corresponded to observations over SB7B site (i.e., lower stand density, unmodified background) with $\Phi = 29^\circ$. The retrieved background reflectance changes with increasing canopy foliage this time (Fig. 9). Illustrated with simulations for the red band, the results indicate the algorithm performs well for low to intermediate stand densities—that is, the situation when the background reflectance does have an important contribution to the total reflectance of the canopy—but with increasing canopy foliage, the error is progressively increasing.

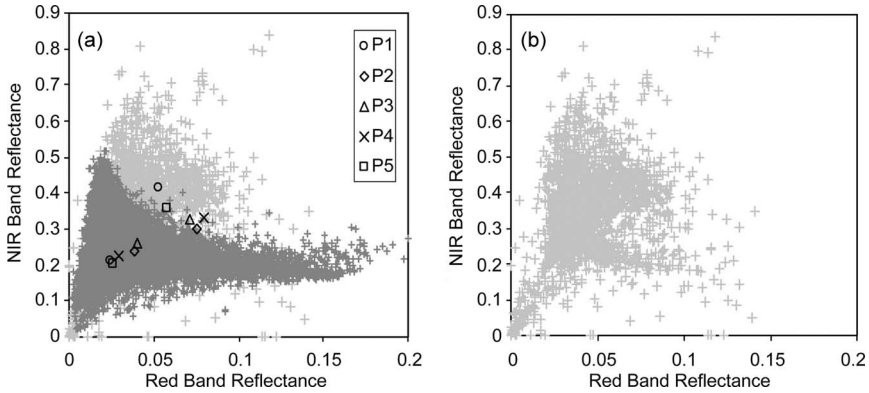

Fig. 7. (a) Distribution of (dark gray) the total reflectances and (light gray) calculated background reflectances for the pixels in the CASI background reflectance map over a subset area of the scene from Fig. 2, near Sudbury, ON, Canada. The highlighted points indicate the differences between the total and background reflectances for the sites from Table III. For clarity, calculated background reflectances only are shown in (b).

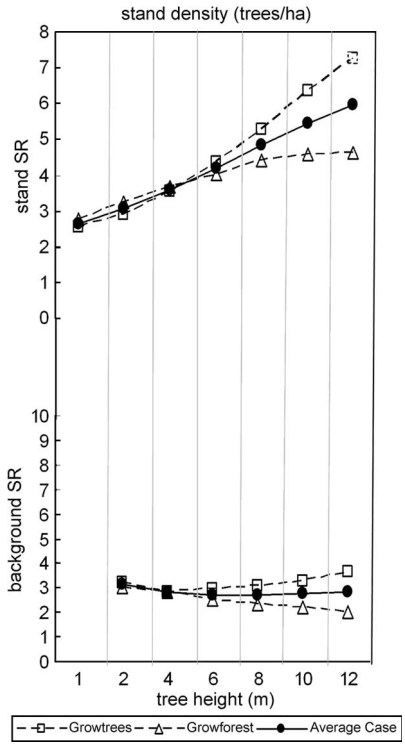

Fig. 8. Changes in SR of 4-Scale simulated scene components with increasing LAI/vertically projected crown area by altering tree size/stand density. Line "Grow trees" corresponds to results achieved with constant stand density and increasing tree size (lower x-axis or Table IV); line "Grow forest" corresponds to results achieved by keeping tree dimensional parameters constant while increasing the stand density (upper x-axis or Table IV). Line "Average case" represents the mean value between the two scenarios at each step.

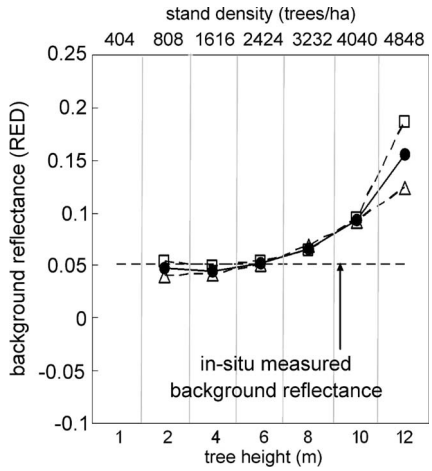

Fig. 9. Sensitivity of the background reflectance estimates to the input stand parameters. The 4-Scale model calculated the scene background components as tree size/stand density increased, while the stand reflectance was kept constant as observed over SB-7 site by CASI. For the legend explanation, see Fig. 8.

If the assumed canopy foliage was twice the amount observed in the field, PE reached up to 100% in the red band. This is not very encouraging. However, one has to bear in mind that in these cases of dense vegetation canopies, LAI is greater than five. A high accuracy of the background retrievals for dense canopies is not possible due to low visibility of the understory through the dense canopy [12], [61], [65], and the role of the background understory is then also not so critical. The stand reflectance at high LAI values is nearly independent of view directions, and, as mentioned, the background has only a very small contribution to the total forest reflectance [66]–[68]. The background plays important role mainly at low to intermediate stand densities, and the results in Fig. 9 indicate the algorithm is less sensitive to the input stand parameters in this domain. As the main purpose for our background reflectance is to improve LAI mapping which is only sensitive to the background when the LAI is small, this expected limitation in our methodology therefore does not defeat our goal of using multiangle data for LAI mapping.

V. Conclusion

This investigation offers new insights into the possibilities and limitations of multiangle data use for estimating the forest background reflectance with a GO model. Through an intensive field campaign including multiangle airborne remote sensing and concurrent ground measurements in forest stands with modified and natural backgrounds, we validated, for the first time, our background reflectance retrieval algorithm. While other authors noted multiangular data can reduce the effect of understory [46], [63], we show that under appropriate zenith and azimuth angular sensor configuration, we can achieve the opposite as well—the retrieval of the signal from forest background. We demonstrated that it is feasible to retrieve the background reflectance with two-angle remote sensing: one at nadir and the other at an off-nadir angle. Although the off-nadir

TABLE IV
OVERVIEW OF INPUT PARAMETERS FOR THE SENSITIVITY ANALYSIS OF THE PREDICTED BACKGROUND REFLECTANCE TO INPUT STAND PARAMETERS

	scenario A (constant stand density 2000 trees/ha)				scenario B
Scenario number	tree height (m)	crown depth (m)	crown radius (m)	vertical projected crown area (m^2)	corresponding stand density (trees/ha)
1	1	0.85	0.34	713.64	404
2	2	1.70	0.48	1427.27	808
3	4	3.39	0.67	2854.55	1616
4	6	5.09	0.83	4281.82	2424
5	8	6.79	0.95	5709.09	3232
6	10	8.48	1.07	7136.36	4040
7	12	10.18	1.17	8563.64	4848

remote sensing is theoretically optimal on the plane perpendicular to the solar plane, our current study shows that the retrieval can also be successful if the background reflectance directionality is considered in the retrieval algorithm.

Several studies have proposed the inclusion of the measurement of the understory component into the canopy LAI algorithms [69]. While the understory LAI measurements are part of the field protocol, for example, for the VALERI group [70] or other networks [71], the information about the forest understory has not been retrieved from remote sensing data. The previous progress in retrieving soil-background responses by [28] and [45] focused on grass- and shrub-dominated areas and the acquired results cannot be simply extrapolated into the forest domain. In this sense, we have made one step forward in retrieving the forest background information from remote sensing data.

However, the successful retrieval also depends on the estimation of various scene fractions used in the algorithm. These scene fractions not only depend strongly on the LAI, which is a required input to the algorithm, but also depend on other stand parameters, such as stand density and tree size. As these parameters are often lacking for large regions, we conducted sensitivity tests of our model, and demonstrated that for low and moderate density stands with LAI < 5, the error in the retrieved background reflectance would be within 16% in the red band and 12% in the NIR band. These results suggest that it is feasible to retrieve the background information from two angle remote sensing with only LAI as the additional input. Our next goal is to apply this algorithm over large areas with MISR data [31], which provide satellite observations at multiple viewing and illumination angles. This paper has provided, in addition to the necessary validation of the theory with airborne and *in situ* measurements, an insight into the sources of uncertainties affecting the performance of the algorithm that will need to be taken in account for large area mapping. Once the seasonal variations of the background optical properties can be retrieved from remote sensing, our regional and global LAI mapping can be significantly improved.

ACKNOWLEDGMENT

The authors would like to thank J. Suomalainen and T. Hakala for carrying out the BRDF measurements of the plastic sheets with Finnish Geodetic Institute Field Goniospectrometer in spring 2008. J. Pisek would like to thank T. Nilson and A. Kuusk of Tartu Observatory, Toravere, Estonia; M. Rautiainen and P. Stenberg from the University of Helsinki; and L. Korhonen of the University of Joensuu, Finland, for useful discussions related to results in this paper during the author's visit to their institutes. The authors would also like to L. E. Quinn for helping with the English style corrections and to anonymous reviewers who helped to improve this paper.

REFERENCES

[1] F. Baret, "CEOS/LPV workshop on LAI & fAPAR validation," presented at CEOS/LPV-VALERI Workshop, Davos, Switzerland, Mar. 2007.
[2] J. M. Chen and T. A. Black, "Defining leaf area index for non-flat leaves," *Plant Cell Environ.*, vol. 15, no. 4, pp. 421–429, 1992.
[3] P. J. Sellers, D. A. Randall, G. J. Collatz, J. A. Berry, C. B. Field, D. A. Dazlich, C. Zhang, G. D. Collelo, and L. Bounoua, "A revised land surface parameterization (SIB2) for atmospheric GCMs. Part I: Model formulation," *J. Clim.*, vol. 9, no. 4, pp. 676–705, Apr. 1996.
[4] R. B. Myneni, S. Hoffman, Y. Knyazikhin, J. L. Privette, J. Glassy, Y. Tian, Y. Wang, X. Song, Y. Zhang, G. R. Smith, A. Lotsch, M. Friedl, J. T. Morisette, P. Votava, R. R. Nemani, and S. W. Running, "Global products of vegetation leaf area and fraction absorbed PAR from one year of MODIS data," *Remote Sens. Environ.*, vol. 83, no. 1/2, pp. 214–231, Nov. 2002.
[5] A. Kuusk, "A two-layer canopy reflectance model," *J. Quant. Spectrosc. Radiat. Transf.*, vol. 71, no. 1, pp. 1–9, Oct. 2001.
[6] L. J. Brown, J. M. Chen, S. G. Leblanc, and J. Cihlar, "Short wave infrared correction to the simple ratio: An image and model analysis," *Remote Sens. Environ.*, vol. 71, no. 1, pp. 16–25, Jan. 2000.
[7] L. Eklundh, K. Hall, H. Eriksson, J. Ardö, and P. Pilesjö, "Investigating the use of Landsat thematic mapper data for estimation of forest leaf area index in Southern Sweden," *Can. J. Remote Sens.*, vol. 29, no. 3, pp. 349–362, 2003.
[8] S. Garrigues, R. Lacaze, F. Baret, J. T. Morisette, M. Weiss, J. E. Nickeson, R. Fernandes, S. Plummer, N. V. Shabanov, R. B. Myneni, Y. Knyazikhin, and W. Yang, "Validation and intercomparison of global leaf area index products derived from remote sensing data," *J. Geophys. Res.*, vol. 113, no. G2, p. G02 028, Jun. 2008. DOI:10.1029/2007JG000635.
[9] J. Pisek, J. M. Chen, and F. Deng, "Assessment of a global leaf area index product from SPOT-4 VEGETATION data over selected sites in Canada," *Can. J. Remote Sens.*, vol. 33, no. 4, pp. 341–356, Aug. 2007.
[10] M. Rautiainen, "Retrieval of leaf area index for a coniferous forest by inverting a forest reflectance model," *Remote Sens. Environ.*, vol. 99, no. 3, pp. 295–303, Nov. 2005.
[11] P. Stenberg, M. Rautiainen, T. Manninen, P. Voipio, and H. Smolander, "Reduced simple ratio better than NDVI for estimating LAI in Finnish pine and spruce stands," *Silva Fenn.*, vol. 38, no. 1, pp. 3–14, 2004.
[12] M. Lang, T. Nilson, A. Kuusk, A. Kiviste, and M. Hordo, "The performance of foliage mass and crown radius models in forming the input of a forest reflectance model: A test on forest growth sample plots and Landsat 7 ETM+ images," *Remote Sens. Environ.*, vol. 110, no. 4, pp. 445–457, Oct. 2007.
[13] M. Rautiainen and P. Stenberg, "Application of photon recollision probability in coniferous canopy reflectance simulations," *Remote Sens. Environ.*, vol. 96, no. 1, pp. 98–107, May 2005.
[14] M. J. Chopping, L. H. Su, A. Rango, and C. Maxwell, "Modelling the reflectance anisotropy of Chihuahuan Desert grass-shrub transition canopy-soil complexes," *Int. J. Remote Sens.*, vol. 25, no. 14, pp. 2725–2745, 2004.
[15] J. M. Chen, G. Pavlic, L. Brown, J. Cihlar, S. G. Leblanc, H. P. White, R. J. Hall, D. R. Peddle, D. J. King, J. A. Trofymow, E. Swift, J. Van der Sanden, and P. K. E. Pellikka, "Derivation and validation of Canada-wide coarse-resolution leaf area index maps using high-resolution

satellite imagery and ground measurements," *Remote Sens. Environ.*, vol. 80, no. 1, pp. 165–184, Apr. 2002.
[16] F. Gemmell, "Testing the utility of multi-angle spectral data for reducing the effects of background spectral variations in forest reflectance model inversion," *Remote Sens. Environ.*, vol. 72, no. 1, pp. 46–63, Apr. 2000.
[17] A. Kuusk and T. Nilson, "A directional multispectral forest reflectance model," *Remote Sens. Environ.*, vol. 72, no. 2, pp. 244–252, May 2000.
[18] S. Dangel, M. M. Verstraete, J. Schopfer, M. Kneubuehler, M. Schaepman, and K. I. Itten, "Toward a direct comparison of field and laboratory goniometer measurements," *IEEE Trans. Geosci. Remote Sens.*, vol. 43, no. 11, pp. 2666–2675, Nov. 2005.
[19] M. J. Chopping, A. Rango, K. M. Havstad, F. R. Schiebe, J. C. Ritchie, T. J. Schmugge, A. N. French, L. Su, L. McKee, and M. R. Davis, "Canopy attributes of desert grassland and transition communities derived from multiangular airborne imagery," *Remote Sens. Environ.*, vol. 85, no. 3, pp. 339–354, May 2003.
[20] A. Kuusk, M. Lang, and T. Nilson, "Simulation of the reflectance of ground vegetation in sub-boreal forests," *Agric. For. Meteorol.*, vol. 126, no. 1/2, pp. 33–46, Nov. 2004.
[21] J. I. Peltoniemi, S. Kaasalainen, J. Näränen, M. Rautiainen, P. Stenberg, H. Smolander, S. Smolander, and P. Voipio, "BRDF measurement of understory vegetation in pine forests: Dwarf shrubs, lichen, and moss," *Remote Sens. Environ.*, vol. 94, no. 3, pp. 343–354, Feb. 2005.
[22] J. L. Bubier, B. N. Rock, and P. M. Crill, "Spectral reflectance measurements of boreal wetland and forest mosses," *J. Geophys. Res.*, vol. 102, no. D24, pp. 29 483–29 494, Dec. 1997.
[23] O. Sonnentag, J. M. Chen, D. A. Roberts, J. Talbot, K. Q. Halligan, and A. Govind, "Mapping tree and shrub leaf area indices in an ombrotrophic peatland through multiple endmember spectral unmixing," *Remote Sens. Environ.*, vol. 109, no. 3, pp. 342–360, Aug. 2007.
[24] F. Deng, J. M. Chen, S. Plummer, M. Z. Chen, and J. Pisek, "Algorithm for global leaf area index retrieval using satellite imagery," *IEEE Trans. Geosci. Remote Sens.*, vol. 44, no. 8, pp. 2219–2229, Aug. 2006.
[25] J. Pisek and J. M. Chen, "Comparison and validation of MODIS and VEGETATION global LAI products over four BigFoot sites in North America," *Remote Sens. Environ.*, vol. 109, no. 1, pp. 81–94, Jul. 2007.
[26] M. Chopping, "Terrestrial applications of multiangle remote sensing," in *Advances in Land Remote Sensing: System, Modeling, Inversion and Applications*, S. Liang, Ed. Berlin, Germany: Springer-Verlag, 2008, pp. 95–144.
[27] F. Canisius and J. M. Chen, "Retrieving forest background reflectance in a boreal region from Multi-Angle Imaging SpectroRadiometer (MISR) data," *Remote Sens. Environ.*, vol. 107, no. 1/2, pp. 312–321, Mar. 2007.
[28] M. J. Chopping, L. H. Su, A. Laliberte, A. Rango, D. Peters, and N. Kollikkathara, "Mapping shrub abundance in desert grasslands using geometric-optical modeling and multi-angle remote sensing with CHRIS/Proba," *Remote Sens. Environ.*, vol. 104, no. 1, pp. 62–73, Sep. 2006.
[29] J. M. Chen and S. G. Leblanc, "A four-scale bidirectional reflectance model based on canopy architecture," *IEEE Trans. Geosci. Remote Sens.*, vol. 35, no. 5, pp. 1316–1337, Sep. 1997.
[30] S. G. Leblanc, P. Bicheron, J. M. Chen, M. Leroy, and J. Cihlar, "Investigation of directional reflectance in boreal forests with an improved four-scale model and airborne POLDER data," *IEEE Trans. Geosci. Remote Sens.*, vol. 37, no. 3, pp. 1396–1414, May 1999.
[31] D. J. Diner, J. C. Beckert, T. H. Reilly, C. J. Bruegge, J. E. Conel, R. A. Kahn, J. V. Martonchik, T. P. Ackerman, R. Davies, S. A. W. Gerstl, H. R. Gordon, J.-P. Muller, R. B. Myneni, P. J. Sellers, B. Pinty, and M. M. Verstraete, "Multi-angle imaging spectro-radiometer (MISR) instrument description and experiment overview," *IEEE Trans. Geosci. Remote Sens.*, vol. 36, no. 4, pp. 1072–1087, Jul. 1998.
[32] J. M. Chen, X. Li, T. Nilson, and A. Strahler, "Recent advances in geometrical optical modelling and its applications," *Remote Sens. Rev.*, vol. 18, no. 2–4, pp. 227–262, Dec. 2000.
[33] X. W. Li and A. H. Strahler, "Geometric-optical modeling of a conifer forest canopy," *IEEE Trans. Geosci. Remote Sens.*, vol. GRS-23, no. 5, pp. 705–721, Sep. 1985.
[34] C. Bacour and F.-M. Bréon, "Variability of biome reflectance directional signatures as seen by POLDER," *Remote Sens. Environ.*, vol. 98, no. 1, pp. 80–95, Sep. 2005.
[35] D. W. Deering, T. F. Eck, and B. Banerjee, "Characterization of the reflectance aniostropy of three boreal forest canopies in spring–summer," *Remote Sens. Environ.*, vol. 67, no. 2, pp. 205–229, Feb. 1999.
[36] S. Kaasalainen and M. Rautiainen, "Hot spot reflectance signatures of common boreal lichens," *J. Geophys. Res.*, vol. 110, no. D20, p. D20 102, Oct. 2005. DOI:10.1029/2005JD005834.
[37] S. Sandmeier, "Variability of BRDF," in *Reflection Properties of Vegetation and Soil—With a BRDF Data Base*, M. von Schönermark, B. Geiger, and H. P. Röser, Eds. Berlin, Germany: Wissenschaft und Technik Verlag, 2004, ch. 3, pp. 131–173.
[38] P. H. White, J. R. Miller, and J. M. Chen, "Four-scale linear model for anisotropic reflectance (FLAIR) for plant canopies. I: Model description and partial validation," *IEEE Trans. Geosci. Remote Sens.*, vol. 39, no. 5, pp. 1073–1083, May 2001.
[39] P. H. White, J. R. Miller, and J. M. Chen, "Four-scale linear model for anisotropic reflectance (FLAIR) for plant canopies—Part II: Validation and inversion with CASI, POLDER and PARABOLA data at BOREAS," *IEEE Trans. Geosci. Remote Sens.*, vol. 40, no. 5, pp. 1038–1046, May 2002.
[40] P. H. White, J. C. Deguise, J. Schwartz, R. Hitchcock, and K. Staenz, "Defining shaded spectra by model inversion for spectral unmixing of hyperspectral datasets—Theory and preliminary application," in *Proc. IEEE IGARSS*, 2002, pp. 989–991.
[41] J. M. Chen and S. G. Leblanc, "A geometrical multiple scattering scheme to be used in geometrical optical models," *IEEE Trans. Geosci. Remote Sens.*, vol. 39, no. 5, pp. 1061–1071, May 2001.
[42] J. Neyman, "On a new class of 'contagious' distribution applicable in entomology and bacteriology," *Ann. Math. Stat.*, vol. 10, pp. 35–57, 1939.
[43] M. Disney, P. Lewis, and P. Saich, "3D modelling of forest canopy structure for remote sensing simulations in the optical and microwave domains," *Remote Sens. Environ.*, vol. 100, no. 1, pp. 114–132, Jan. 2006.
[44] Y. Zhang, J. M. Chen, J. R. Miller, and T. L. Noland, "Leaf chlorophyll content retrieval from airborne hyperspectral remote imagery," *Remote Sens. Environ.*, vol. 112, no. 7, pp. 3234–3247, Jul. 2008.
[45] M. J. Chopping, L. Su, A. Rango, J. V. Martonchik, D. P. C. Peters, and A. Laliberte, "Remote sensing of woody shrub cover in desert grasslands using MISR with a geometric-optical canopy reflectance model," *Remote Sens. Environ.*, vol. 112, no. 1, pp. 19–34, Jan. 2008.
[46] J. Heiskanen, "Tree cover and height estimation in the Fennoscandian tundra–taiga transition zone using multiangular MISR data," *Remote Sens. Environ.*, vol. 103, no. 1, pp. 97–114, Jul. 2006.
[47] M. J. Hill, C. Averill, Z. Jiao, C. B. Schaaf, and J. D. Armston, "Relationship of MISR RPV parameters and MODIS BRDF shape indicators to surface vegetation patterns in an Australian tropical savanna," *Can. J. Remote Sens.*, vol. 34, pp. 247–267, 2008. suppl. 2.
[48] M. A. Schull, S. Ganguly, A. Samanta, D. Huang, N. V. Shabanov, J. P. Jenkins, J. C. Chiu, A. Marshak, J. B. Blair, R. B. Myneni, and Y. Knyazikhin, "Physical interpretation of the correlation between multi-angle spectral data and canopy height," *Geophys. Res. Lett.*, vol. 34, no. 18, p. L18 405, Sep. 2007. DOI:10.1029/2007GL031143.
[49] J. M. Chen, A. Govind, O. Sonnentag, Y. Zhang, A. Barr, and B. Amiro, "Leaf area index measurements at Fluxnet-Canada forest sites," *Agric. For. Meteorol.*, vol. 140, no. 1–4, pp. 257–268, Nov. 2006.
[50] J. M. Chen and J. Cihlar, "Plant canopy gap-size analysis theory for improving optical measurements of leaf-area index," *Appl. Opt.*, vol. 34, no. 27, pp. 6211–6222, Sep. 1995.
[51] S. G. Leblanc, "Correction to the plant canopy gap size analysis theory used by the tracing radiation and architecture of canopies (TRAC) instrument," *Appl. Opt.*, vol. 41, no. 36, pp. 7667–7670, Sep. 2002.
[52] S. T. Gower, C. J. Kucharik, and J. M. Norman, "Direct and indirect estimation of leaf area index, f_{APAR}, and net primary production of terrestrial ecosystems," *Remote Sens. Environ.*, vol. 70, no. 1, pp. 29–51, Oct. 1999.
[53] J. Suomalainen, J. Peltoniemi, T. Hakala, and E. Puttonen, "Finnish Geodetic Institute Field Goniospectrometer (FIGIFIGO): A device for polarized multiangular reflectance measurements," in *Proc. IEEE IGARSS*, Jul. 2008. CD-ROM.
[54] D. Haboudane, N. Tremblay, J. R. Miller, and P. Vigneault, "Remote estimation of crop chlorophyll content using spectral indices derived from hyperspectral data," *IEEE Trans. Geosci. Remote Sens.*, vol. 46, no. 2, pp. 423–437, Feb. 2008.
[55] J. S. Iiames, A. N. Pilant, T. E. Lewis, and R. Congalton, "Leaf area index (LAI) change detection on loblolly pine forest stands with complete understory removal," in *Proc. Annu. Amer. Soc. Photogramm. Remote Sens.*, Denver, CO, 2004.
[56] S. Sandmeier and K. Itten, "A field goniometer system (FIGOS) for acquisition of hyperspectral BRDF data," *IEEE Trans. Geosci. Remote Sens.*, vol. 37, no. 2, pp. 648–658, Mar. 1999.
[57] W. Ni and X. Li, "A coupled vegetation-soil bidirectional reflectance model for a semiarid landscape," *Remote Sens. Environ.*, vol. 74, no. 1, pp. 113–124, Oct. 2000.

[58] S.-C. Tsay, M. King, G. T. Arnold, and J. Y. Li, "Airborne spectral measurements of surface anisotropy using SCAR-B," *J. Geophys. Res.*, vol. 103, no. D24, pp. 31 943–31 953, 1998.
[59] A. Kokhanovsky, T. Aoki, A. Hachikubo, M. Hori, and E. P. Zege, "Reflective properties of natural snow: Approximate asymptotic theory versus in situ measurements," *IEEE Trans. Geosci. Remote Sens.*, vol. 43, no. 7, pp. 1529–1535, Jul. 2005.
[60] J. Pisek, J. M. Chen, J. R. Miller, and J. Peltoniemi, "Mapping of forest background reflectance over North America with MISR," in *Proc. MISR Data Users Sci. Symp.*, Pasadena, CA, Dec. 2008.
[61] H. Eriksson, L. Eklundh, A. Kuusk, and T. Nilson, "Impact of understory vegetation on forest canopy reflectance and remotely sensed LAI estimates," *Remote Sens. Environ.*, vol. 103, no. 4, pp. 408–418, Aug. 2006.
[62] A. Simic, J. M. Chen, J. Freemantle, J. R. Miller, and J. Pisek, "Improving clumping and LAI algorithms based on multi-angle airborne imagery and ground measurements," *IEEE Trans. Geosci. Remote Sens.*, to be published.
[63] M. Rautiainen, M. Lang, M. Mottus, A. Kuusk, T. Nilson, J. Kuusk, and T. Lukk, "Multi-angular reflectance properties of a hemiboreal forest: An analysis using CHRIS PROBA data," *Remote Sens. Environ.*, vol. 112, no. 5, pp. 2627–2642, May 2008.
[64] S. Sandmeier and D. W. Deering, "Structure analysis and classification of boreal forests using airborne hyperspectral BRDF data from ASAS," *Remote Sens. Environ.*, vol. 69, no. 3, pp. 281–295, Sep. 1999.
[65] T. Nilson, "Inversion of gap frequency data in forest stands," *Agric. For. Meteorol.*, vol. 98/99, pp. 437–448, Dec. 1999. Special Issue.
[66] R. K. Kaufmann, L. Zhou, Y. Knyazikhin, N. V. Shabanov, R. B. Myneni, and C. J. Tucker, "Effect of orbital drift and sensor changes on the time series of AVHRR vegetation index data," *IEEE Trans. Geosci. Remote Sens.*, vol. 38, no. 6, pp. 2584–2597, Nov. 2000.
[67] P. J. Zarco-Tejada, J. R. Miller, T. L. Noland, G. H. Mohammed, and P. H. Sampson, "Scaling-up and model inversion methods with narrowband optical indices for chlorophyll content estimation in closed forest canopies with hyperspectral data," *IEEE Trans. Geosci. Remote Sens.*, vol. 39, no. 7, pp. 1491–1507, Jul. 2001.
[68] Y. Zhang, N. V. Shabanov, Y. Knyazikhin, and R. B. Myneni, "Assessing the information content of multiangle satellite data for mapping biomes. II. Theory," *Remote Sens. Environ.*, vol. 80, no. 3, pp. 435–446, Jun. 2002.
[69] J. T. Morisette, F. Baret, J. L. Privette, R. B. Myneni, J. E. Nickeson, S. Garrigues, N. V. Shabanov, M. Weiss, R. A. Fernandes, S. G. Leblanc, M. Kalacska, G. A. Sanchez-Azofeifa, M. Chubey, B. Rivard, P. Stenberg, M. Rautiainen, P. Voipio, T. Manninen, A. N. Pilant, T. E. Lewis, J. S. Iiames, R. Colombo, M. Meroni, L. Busetto, W. B. Cohen, D. P. Turner, E. D. Warner, G. W. Petersen, G. Seufert, and R. Cook, "Validation of global moderate-resolution LAI products: A framework proposed within the CEOS land product validation subgroup," *IEEE Trans. Geosci. Remote Sens.*, vol. 44, no. 7, pp. 1804–1817, Jul. 2006.
[70] VALERI, *Validation of Land European Remote Sensing Instruments Network*, 2007. [Online]. Available: http://www.avignon.inra.fr/valeri/
[71] F. Baret, J. Morisette, R. A. Fernandes, J. L. Champeaux, R. B. Myneni, J. Chen, S. Plummer, M. Weiss, C. Bacour, S. Garrigues, and J. E. Nickeson, "Evaluation of the representativeness of networks of sites for the global validation and intercomparison of land biophysical products: Proposition of the CEOS-BELMANIP," *IEEE Trans. Geosci. Remote Sens.*, vol. 44, no. 7, pp. 1794–1803, Jul. 2006.

Jan Pisek received the M.Sc. degree in geoinformatics and cartography from Masaryk University, Brno, Czech Republic, in 2004 and the M.Sc. degree in physical geography from the University of Toronto, Toronto, ON, Canada, in 2005, where he is currently working toward the Ph.D. degree.

He is also currently with the Tartu Observatory, Toravere, Estonia. His work deals with the retrieval of vegetation background reflectance and clumping index and their incorporation in the global vegetation models. His research interests cover *in situ* and remote sensing vegetation structure retrieval, with multiangle data in particular.

Jing M. Chen received the B.Sc. degree in applied meteorology from the Nanjing Institute of Meteorology, Nanjing, China, in 1982 and the Ph.D. degree in meteorology from Reading University, Reading, U.K., in 1986.

From 1989 to 1993, he was a Postdoctoral Fellow and Research Associate with the University of British Columbia, Vancouver, BC, Canada. From 1993 to 2000, he was a Research Scientist with the Canada Centre for Remote Sensing, Ottawa, ON, Canada. He is currently a Professor and a Canada Research Chair with the Department of Geography, University of Toronto, Toronto, ON, and an Adjunct Professor with York University, Toronto, ON, Canada. He has published over 160 papers in refereed journals. His recent research interests are in the remote sensing of biophysical parameters, plant canopy radiation modeling, terrestrial water and carbon cycle modeling, and atmospheric inverse modeling for global and regional carbon budget estimation.

Dr. Chen is a Fellow of the Royal Society of Canada and Senior Canada Research Chair. He served as an Associate Editor of the IEEE TRANSACTIONS ON GEOSCIENCE AND REMOTE SENSING from 1996 to 2002.

John R. Miller received the B.E. degree in physics and the M.Sc. and Ph.D. degrees in space physics from the University of Saskatchewan, Saskatoon, SK, Canada, in 1963, 1966, and 1969, respectively.

He spent two years on a postdoctoral fellowship with the Herzberg Institute, National Research Council, Ottawa, ON, Canada. Since 1972, he has been with York University, Toronto, ON, Canada, where he was a Professor of physics and earth and space science until his retirement in 2008. His remote sensing interests include atmospheric correction and extraction of biophysical surface parameters through radiative transfer models from water color reflectance and from canopy reflectance for forestry and agriculture applications. Over the past two decades, his primary focus has been on the application of reflectance spectroscopic techniques in remote sensing using imaging spectrometer sensors.

James R. Freemantle received the B.Sc. degree in physics from the University of Waterloo, Waterloo, ON, Canada, and the M.Sc. degree in physics from York University, Toronto, ON, Canada.

Since 1990, he has been a Project Scientist with the Earth Observations Laboratory, Centre for Research in Earth and Space Technology, York University. His research interests include atmospheric correction of airborne and satellite imagery, software development for the processing of airborne imagery from Compact Airborne Spectrographic Imagers, and real-time analysis of remote sensing data.

Jouni I. Peltoniemi received the Ph.D. degree in theoretical physics from the University of Helsinki, Helsinki, Finland, in 1993.

He is currently a Researcher with the Finnish Geodetic Institute, Masala, Finland.

Anita Simic received the M.Sc. degree from the University of Toronto, Toronto, ON, Canada, where she is currently working toward the Ph.D. degree in the Department of Geography.

In 2002–2005, she was as an Intermediate Research Scientist with the Canada Centre for Remote Sensing. She is currently a Sessional Instructor with the University of Toronto and Ryerson University, Toronto, ON, Canada, where she has been teaching remote sensing and GIS courses since 2005.